

A computational study of stereospecificity in the thermal elimination reaction of menthyl benzoate in the gas phase

Ederley Vélez^{a*}, Jairo Quijano^a, Rafael Notario^b, Elizabeth Pabón^a, Juliana Murillo^a, Julieth Leal^a, Edilma Zapata^a and Gustavo Alarcón^a



This paper reports a theoretical study, at the B3LYP/6-31 + G(d,p) and M05-2X/6-31G + (d,p) levels, on the thermal decomposition of menthyl benzoate (2-isopropyl-5-methylcyclohexyl benzoate). It undergoes a unimolecular first-order elimination to give 3-menthene (1-isopropyl-4-methylcyclohexene), 2-menthene (3-isopropyl-6-methylcyclohexene), and benzoic acid. We studied two possible mechanisms trying to explain the formation of 2- and 3-menthene, via six-membered or four-membered cyclic transition states. Rate constants were calculated at two temperatures, 587.1 and 598.6 K, and they agree well with the experimentally determined values. We verify that 3-menthene is the product mainly formed at both temperatures. The progress of the reactions has been followed by means of the Wiberg bond indices. Intrinsic reaction coordinate (IRC) calculations have been carried out to verify that the localized transition state structures connect with the reactants and products and also to verify that the parent compound, menthyl benzoate, is taking the *cis*-configuration needed in the reaction. Copyright © 2009 John Wiley & Sons, Ltd.

Supplementary information may be found in the online version of this paper.

Keywords: B3LYP; DFT; Intrinsic reaction coordinate (IRC); M05-2X; menthyl benzoate; reaction mechanism; thermal decomposition

INTRODUCTION

The thermal decomposition of esters to produce olefins and carboxylic acids is a reaction which is frequently of preparative value, and it has been studied since 1883.^[1] The esters that undergo pyrolysis may be divided into two classes: esters with β -hydrogen atoms on the alkyl portion of the molecule and esters without β -hydrogen atoms. Although some workers^[2] believe that all esters decompose thermally by the same mechanism, others^[3] believe that the mechanism is not the same in the two cases. They base their belief on the contrasting conditions of pyrolysis and the resulting products. Pyrolysis of esters without β -hydrogens in the alkyl portion requires higher temperatures and the products are suggestive of a free radical type mechanism.^[3] However, if β -hydrogen atoms are available and the temperature of pyrolysis is optimum, only the expected olefins and acids result. Only esters belonging to the latter class were studied in this investigation.

There is an important type of elimination mechanism which is chemically specific in the *cis*-sense. The mechanism is illustrated by those olefins giving thermal decomposition reactions which occur homogeneously and are unimolecular.^[4] Hurd and Blunk^[3] proposed that the esters which contain a β -hydrogen in the alkyl group may undergo a chelate type of six-atom ring closure by a hydrogen bridge i.e., a six-membered transition state. For example, the pyrolysis of ethyl chloride proceeds by a unimolecular mechanism giving hydrogen chloride and the corresponding olefin,^[4] the transition state in this reaction is a specific example of a four-center ring; it is characteristic that the

four-center rings must lie, suitably disposed with respect to each other, in one plane to ensure the minimization of the activation energy and, therefore, *cis*-stereochemistry must be demanded in the reactant. This deduction applies quite generally to unimolecular thermal decomposition reactions.

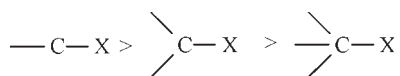
Additional evidence is provided on the stereochemical specificity of Chugaev's xanthate reaction.^[4,5]

In both cases, *cis*-elimination has been feasible, in principle, in a direction away from the bridgehead. It is of interest, therefore, to establish the reason for preferential *cis*-elimination toward the bridgehead when this is stereochemically possible. It is now universally recognized that the homolytic bond dissociation energies of C—X bonds, where X = H, OH, Cl, Br, I, etc. diminish markedly in the series primary, secondary, tertiary. It would be expected, therefore, that unimolecular elimination of H—X should also proceed with decreasing activation energy in the series:

* Correspondence to: E. Vélez, Laboratorio de Fisicoquímica Orgánica, Facultad de Ciencias, Universidad Nacional de Colombia, Sede Medellín, Apartado Aéreo 3840, Medellín, Colombia.
E-mail: evortiz@unalmed.edu.co

a E. Vélez, J. Quijano, E. Pabón, J. Murillo, J. Leal, E. Zapata, G. Alarcón
Laboratorio de Fisicoquímica Orgánica, Facultad de Ciencias, Universidad Nacional de Colombia, Sede Medellín, Apartado Aéreo, Medellín, Colombia

b R. Notario
Instituto de Química Física "Rocasolano", C.S.I.C., Madrid, Spain



Following the study of these reactions, classed as pericyclic processes, we have carried out a study of the pyrolysis of menthyl benzoate (2-isopropyl-5-methylcyclohexyl benzoate, **MB**) to give a mixture of 3-menthene (1-isopropyl-4-methylcyclohexene, **3ENE**), 2-menthene (3-isopropyl-6-methylcyclohexene, **2ENE**), and benzoic acid, **P1**, as shown in Fig. 1. Barton *et al.*^[6] have concluded the reaction is homogeneous and unimolecular in its mechanism. The analysis of the ratio **3ENE:2ENE** olefin produced in the decomposition is approximately 2:1.

In this work, we have tried to identify the stereospecificity of this reaction. The mechanism suggested from the experiments^[2,4,6] for the decomposition process is described in Fig. 2. The products of the reaction suggest that the process should be either via a six-membered cyclic transition state or a four-membered cyclic transition state (as shown in Fig. 2).

COMPUTATIONAL DETAILS

All calculations were carried out using the Gaussian03 computational package.^[7] The geometric parameters for all the reactants, transition states, and products of the reactions studied were fully optimized using density functional theory (DFT)^[8] with B3LYP^[9] and M05-2X^[10] functionals with the 6-31G + (d,p) basis set.^[11]

B3LYP is a combination of Becke's three parameter hybrid exchange functional^[12] with the Lee, Yang, and Parr correlated functional.^[13] The recently reported^[10] M05-2X is a high-nonlocality functional with double the amount of non-local exchange (2X) that is parameterized only for nonmetals and it is based on simultaneously optimized exchange and correlation functionals both including kinetic energy density. It has shown very good performance for applications involving thermochemistry, kinetics, and non-covalent interactions.^[14]

Each structure was characterized as a minimum or a saddle point of first order by analytical frequency calculations. Thermal corrections to enthalpy and entropy values have been evaluated at the experimental temperatures of 587.1 and 598.6 K. To calculate enthalpy and entropy values at a temperature T , the difference between the values at that temperature and 0 K has been evaluated according to standard thermodynamics.^[15]

Intrinsic reaction coordinate (IRC) calculations^[16] have been performed in all cases to verify that the localized transition state structures connect with the corresponding minimum stationary points associated with reactants and products.

The bonding characteristics of the different reactants, transition states, and products have been investigated using a population partition technique, the natural bond orbital (NBO) analysis of Reed and Weinhold.^[17,18] NBO formalism provides values for the atomic natural total charges and also provides the Wiberg bond indices^[19] used to follow the progress of the reactions. The NBO analysis has been performed using the NBO program,^[20] implemented in the Gaussian 03 package.^[7]

We have selected the classical transition state theory (TST)^[21,22] to calculate the kinetic parameters, and using the Eckart correction for tunneling effect along the reaction coordinate. The Eckart method^[23] is a sophisticated approach that involves fitting the reaction coordinate to a so-called Eckart potential, permitting an exact, analytic solution of the probability of tunneling through the barrier (and of non-classical reflection) from the time-independent Schrödinger equation for systems of fixed energy.^[24] It needs potential energy information only at the stationary points, and thus it may be used with the TST formalism.

Combining the Eckart transmission coefficient, $\kappa^E(T)$, with the rate constant calculated using TST, the new rate constant at a temperature T , is calculated as

$$k(T) = \kappa^E(T) k_{\text{TST}}(T) \quad (1)$$

Calculations of Eckart transmission coefficients have been performed using the Virtual Kinetic Laboratory (VKLab) program.^[25]

RESULTS AND DISCUSSION

Theoretical calculations at the B3LYP/6-31 + G(d,p) and M05-2X/6-31 + G(d,p) levels of theory were carried out in order to explore the nature of the reaction mechanism for the unimolecular decomposition of menthyl benzoate (**MB**) in the gas phase, and also to compare the ability of both the DFT methods in kinetic studies.

We have investigated two pathways as shown in Fig. 2. Mechanisms (A) and (C) proceed through six-membered cyclic transition states, in which both the carbonyl (O_2) and the ether (O_4) oxygen atoms are involved, and mechanisms (B) and (D), proceed through four-membered cyclic transition states in which only the ether oxygen atom (O_4) is participating. All the mechanisms produce either **3ENE** or **2ENE**, and benzoic acid.

Electronic energies, E_{el} , zero-point vibrational energies (ZPE), thermal corrections to enthalpies (TCH), and entropies (S), at two temperatures (587.1 and 598.6 K), for the reactants, transition states, and products involved in the reaction studied (as shown in Fig. 2), calculated at the B3LYP/6-31 + G(d,p) and M05-2X/

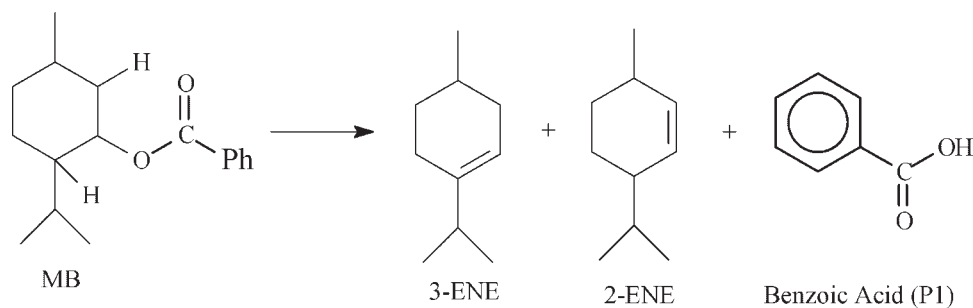


Figure 1. Thermal decomposition of menthyl benzoate, **MB**

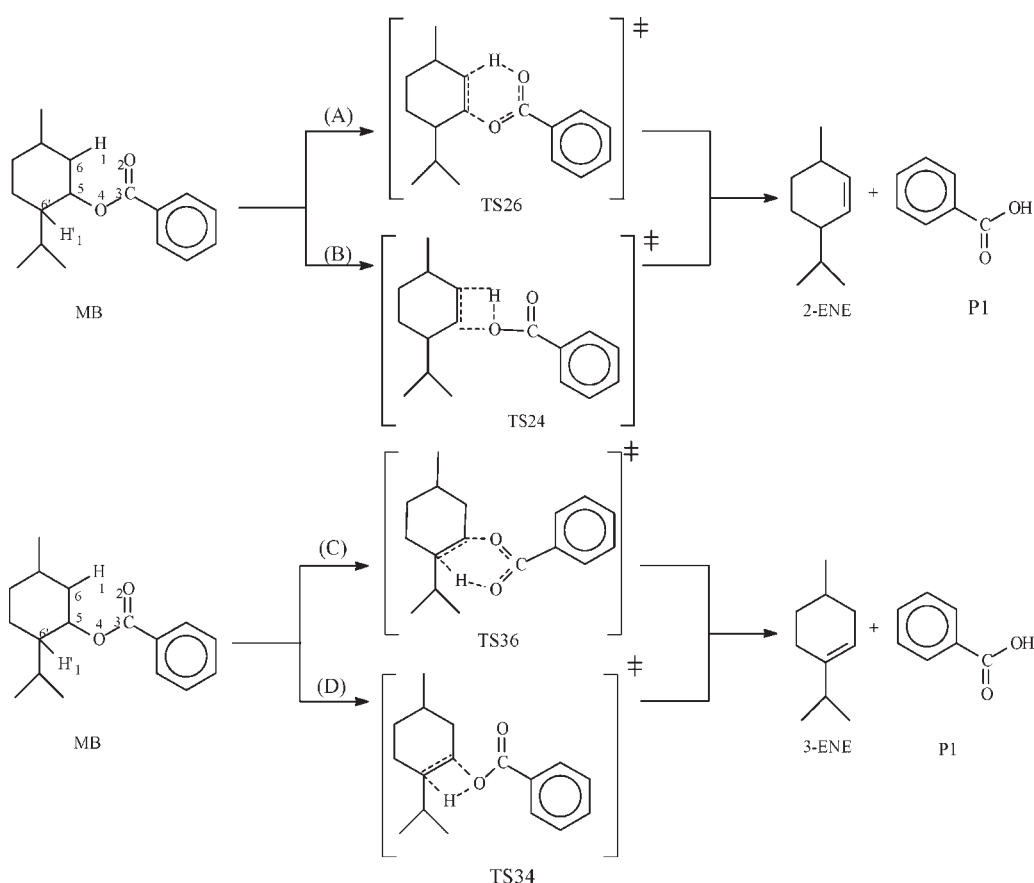


Figure 2. Proposed mechanisms for the thermolysis of menthyl benzoate

6-31 + G(*d,p*) levels of theory, are shown in Table S1 in the Supporting Information. The Cartesian coordinates for all the structures, optimized at the M05-2X/6-31 + G(*d,p*) level, are also collected in Table S2 in the Supporting Information.

Calculated values of the activation parameters and experimental and calculated rate constants for the thermal decomposition of menthyl benzoate, at both DFT levels, are shown in Table 1.

As we have already commented, we found that the reaction of decomposition of **MB** can proceed via two pathways. They are

therefore two competitive reactions, mechanism (A) and (C) through **TS26** and **TS36**, respectively. To obtain the global reaction rate constant, k^{GLO} , we have applied the competitive canonical unified statistical (CCUS) theory,^[27] in which the global reaction rate constant, $k^{\text{GLO}}(T)$ is given by

$$k^{\text{GLO}}(T) = \kappa_{\text{TS36}}^{\text{E}}(T)k^{\text{TS36}}(T) + \kappa_{\text{TS26}}^{\text{E}}(T)k^{\text{TS26}}(T) \quad (2)$$

introducing the transmission coefficient $\kappa^{\text{E}}(T)$ calculated for each mechanism.

Table 1. Calculated^a activation parameters and rate constants for the thermal decomposition of menthyl benzoate at two temperatures, 587.1 K and 598.6 K

T (K)	Mechanism	$\Delta H^{\ddagger}/\text{kJ mol}^{-1}$		$\Delta S^{\ddagger}/\text{J mol}^{-1} \text{K}$		$\Delta G^{\ddagger}/\text{kJ mol}^{-1}$		κ^{E}		$k_{\text{TS}}/\text{s}^{-1}$		$k(\text{exp})^{\text{c}}/\text{s}^{-1}$
		M05-2X	B3LYP ^b	M05-2X	B3LYP	M05-2X	B3LYP ^b	M05-2X	B3LYP	M05-2X	B3LYP ^b	
587.1	(A)	215.2	183.4	7.0	4.0	211.1	181.1	1.505	1.301	2.01×10^{-6}	1.01×10^{-3}	5.7×10^{-4}
	(C)	197.0	169.2	14.6	6.9	188.4	165.2	1.327	1.191	2.08×10^{-4}	2.65×10^{-2}	
									$k^{\text{GLO}}/\text{s}^{-1}$	2.8×10^{-4}	3.3×10^{-2}	
598.6	(A)	215.2	183.5	7.0	3.6	211.0	181.3	1.489	1.292	4.61×10^{-6}	2.05×10^{-3}	1.1×10^{-3}
	(C)	197.0	169.3	14.6	6.6	188.3	165.3	1.318	1.187	4.46×10^{-4}	5.11×10^{-2}	
									$k^{\text{GLO}}/\text{s}^{-1}$	6.0×10^{-4}	6.3×10^{-2}	

^a Values calculated using 6-31+G(*d,p*) basis set.

^b A scaling factor^[26] of 0.9804 for ZPE has been used.

^c Values taken from ref^[6].

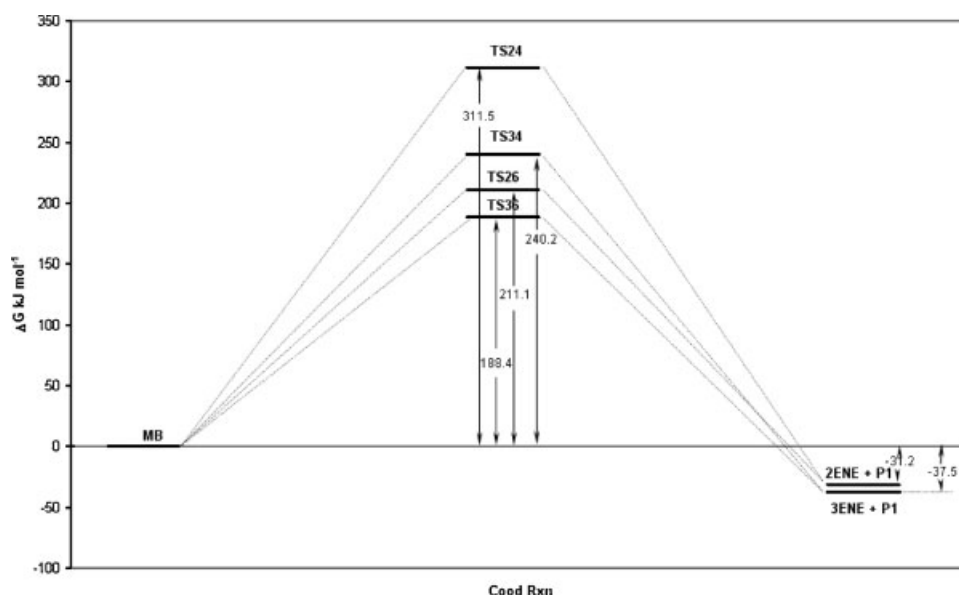


Figure 3. Gibbs energy profile at 587.1 K, evaluated at the M05-2X/6-31 + G(*d,p*) level, for the thermal decomposition of menthyl benzoate

As it can be observed in Table 1, the rate constants calculated using M05-2X functional, are closer to the experimental values. It is known that B3LYP systematically underestimates reaction barrier heights by an average of 18.4 kJ mol^{-1} .^[28] This underestimation is usually ascribed to the self-interaction error (unphysical interaction of an electron with itself) in local DFT. The current study confirms the improved performance of the M05-2X functional as compared to B3LYP.

It is difficult to explain the good agreement between experimental and calculated *k* values, in spite of the calculated activation entropies with positive values. Probably it is due to cancelation errors.

The rate of formation of **2ENE** is lower than that of **3ENE**. It can be attributed to the fact that elimination in this case is predominantly with a tertiary hydrogen atom, whereas in the former case it is with a primary one. The theoretical results agree with the experimental fact that ratio of products **3ENE:2ENE** is approximately 2:1.

Gibbs energy profile for the thermal decomposition process of menthyl benzoate, at a temperature of 587.1 K, is presented in Fig. 3. As it can be observed in this figure, the barriers through **TS34** and **TS24** are higher, and so it is unlikely that the reaction follows these routes. The lowest barrier corresponds to the mechanism (C), i.e., through a six-membered transition state, **TS36**, to obtain **3ENE**. (The Gibbs energy profile at 598.6 K is very similar to this one. It is shown in the Supporting Information, Figure S1). **TS36** is lower in Gibbs energy than **TS26**, according to the experimental evidence: **3ENE** was the product mainly formed at both temperatures. These results confirm that the thermolysis occurs via a mechanism in one step. The processes are highly exergonic.

Figure 4 shows the optimized structures of the transition states, **TS36** and **TS26**, the geometries confirm the *cis*-stereochemistry needed in the reaction. There is one and only one imaginary vibrational frequency in the transition states for the studied thermal decomposition reaction ($781.5i$ and $1021.3i \text{ cm}^{-1}$ for **TS36** and **TS26**, respectively, evaluated at the M05-2X/6-31G + (*d,p*) level of theory, with the lowest real frequencies being 10.8 and 22.1 cm^{-1} for **TS36** and **TS26**, respectively).

IRC calculations have been carried out to verify that the localized transition state structures connect with the reactants and products and also to verify that the parent compound, **MB**, is taking the *cis*-configuration needed in the reaction. Figure 5 shows the IRC for **TS36**. Some structures along the IRC path have been depicted. In structure **1**, the double bond $\text{C}_3\text{—O}_4$ is already formed and the $\text{O}_4\text{—C}_5$ bond has been completely broken. In structure **2**, the H'_1 has begun to be transferred toward O_2 . In structure **3**, after the transition state, the single bond $\text{H}'_1\text{—O}_2$ is almost formed, although the $\text{O}_2\text{—C}_3$ bond is still a double bond. At the end, structure **4** is very similar to the final products.

To avoid the subjective aspects associated with geometrical analysis of the transition states, we have carried out an NBO analysis. The progress of the reaction of decomposition of menthyl benzoate has been followed by means of the Wiberg bond indices, B_{ij} ,^[19] like in other theoretical studies on reaction mechanisms carried out by us.^[29–32] The bond index between two atoms is a measure of the bond order and, hence, of the bond strength between these two atoms, thus, if the evolution of the bond indices corresponding to the bonds being made or broken in a chemical reaction is analyzed along the reaction path, a very precise image of the timing and extent of the bond-breaking and bond-forming processes at every point can be achieved.^[33]

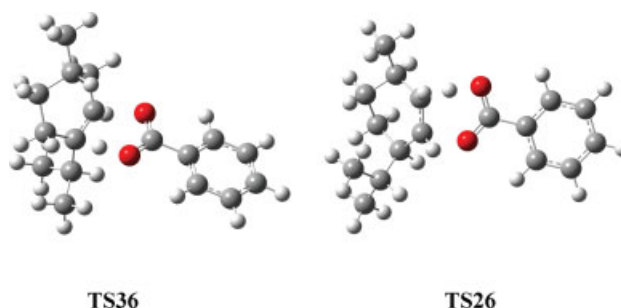


Figure 4. M05-2X/6-31 + G(*d,p*)-optimized transition state structures for the studied reaction

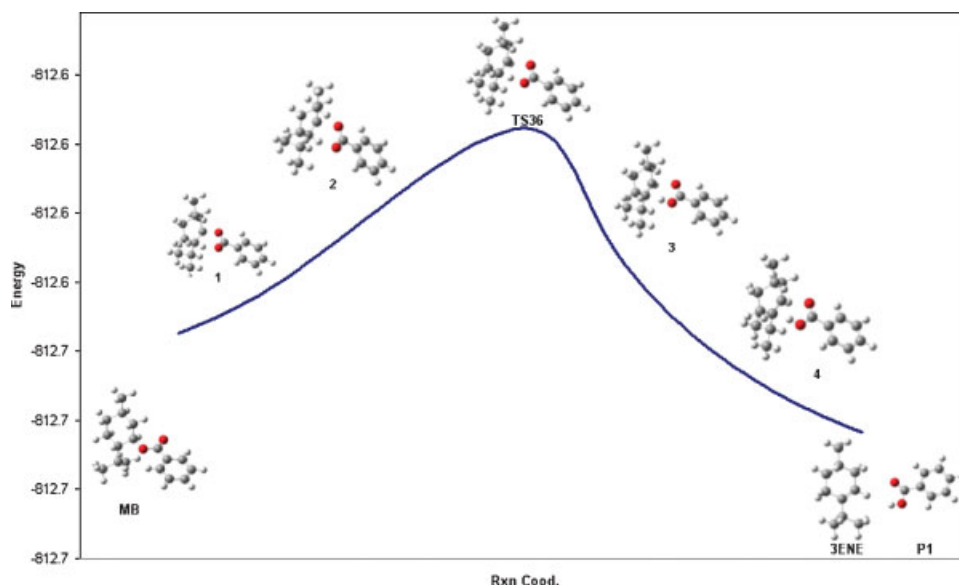


Figure 5. Intrinsic reaction coordinate (IRC) plot from **TS36** toward reactive, menthyl benzoate (**MB**) and toward products, 3-menthene (**3ENE**) and benzoic acid (**P1**)

The Wiberg bond indices, corresponding to the bonds involved in the reaction center of the mechanisms (A) and (C) for all the reactants, transition states, and products, are shown in Table 2.

Moyano *et al.*^[33] have defined a relative variation of the bond index at the transition state, δB_i , for every bond, i , involved in a chemical reaction as

$$\delta B_i = \frac{(B_i^{\text{TS}} - B_i^{\text{R}})}{(B_i^{\text{P}} - B_i^{\text{R}})} \quad (3)$$

where the superscripts R, TS, and P, refer to reactants, transition states, and products, respectively.

The calculated percentages of evolution (%EV = $100\delta B_i$) of the bonds involved in the reaction center are shown in Table 2. As it can be seen, in both mechanisms the breaking of the $\text{O}_4\text{—C}_5$ bond is the most advanced process (63.8 and 63.0% in

mechanisms (A) and (C), respectively), followed by the transformation of the $\text{C}_3\text{—O}_4$ single bond into a double one (*ca* 50%), the $\text{O}_2\text{—C}_3$ double bond into a single one ($\sim 49\%$), and the breaking of the $\text{C}_6\text{—H}_1(\text{H}'_1)$ bond ($\sim 48\%$). The least advanced processes are the formation of the $\text{C}_5\text{—C}_6(\text{C}'_6)$ bond (35.6 and 31.5% in mechanisms (A) and (C), respectively), and the formation of the $\text{H}_1(\text{H}'_1)\text{—O}_2$ single bond (36.1 and 34.0%).

The dissociation of the $\text{C}_5\text{—O}_4$ ($\text{C}_\alpha\text{—X}$) bond before that of the $\text{C}_6\text{—H}_1$ ($\text{C}_\beta\text{—H}$) bond is in accordance with the proposal of Taylor *et al.*^[34,35] for the 1,5 thermal eliminations, based on the fact that the Hammett ρ values at the α -carbon were of larger magnitude than those observed for the β -carbon.

The trend in the degree of bond lengthening can be mirrored using the NBO atomic charges. In Table 3, we have collected the natural atomic charges (the nuclear charges minus the summed

Table 2. Wiberg bond indices, B_i , of reactants, transition states, and products; percentage of evolution through the chemical process of the bond indices at the transition states, %EV; degree of advancement of the transition states, δB_{av} and absolute synchronicities, S_y , for the mechanisms (A) and (C) of the studied reaction^a

Mechanism		$\text{H}_1\text{—O}_2$	$\text{O}_2\text{—C}_3$	$\text{C}_3\text{—O}_4$	$\text{O}_4\text{—C}_5$	$\text{C}_5\text{—C}_6$	$\text{C}_6\text{—H}_1$
(A)	B_i^{R}	0.001	1.701	1.037	0.840	1.001	0.898
	B_i^{TS}	0.250	1.371	1.381	0.304	1.332	0.469
	B_i^{P}	0.691	1.035	1.728	0.000	1.932	0.000
	%EV	36.1	49.5	49.8	63.8	35.6	47.8
		$\delta B_{\text{av}} = 0.47$			$S_y = 0.91$		
		$\text{H}'_1\text{—O}_2$	$\text{O}_2\text{—C}_3$	$\text{C}_3\text{—O}_4$	$\text{O}_4\text{—C}_5$	$\text{C}_5\text{—C}'_6$	$\text{C}'_6\text{—H}'_1$
(C)	B_i^{R}	0.001	1.701	1.037	0.840	1.001	0.898
	B_i^{TS}	0.236	1.379	1.376	0.310	1.294	0.465
	B_i^{P}	0.691	1.035	1.728	0.000	1.932	0.000
	%EV	34.0	48.2	49.1	63.0	31.5	48.2
		$\delta B_{\text{av}} = 0.46$			$S_y = 0.89$		

^a All values calculated at the M05-2X/6-31+G(d,p) level.

Table 3. M05-2X/6-31 + G(d,p)-calculated NBO charges, at the atoms involved in the mechanisms (A) and (C) for the studied reaction^a

	H ₁ (H' ₁)	O ₂	C ₃	O ₄	C ₅	C ₆ (C' ₆)
MB	0.272	-0.630	0.846	-0.575	0.067	-0.501
TS26	0.448	-0.711	0.847	-0.685	0.152	-0.639
MB	0.257	-0.630	0.846	-0.575	0.067	-0.290
TS36	0.453	-0.711	0.840	-0.683	0.148	-0.440

^a As shown in Fig. 2 for atom labeling.

natural populations of the natural atomic orbitals on the atoms) at the atoms involved in the mechanisms (A) and (C) for the studied reaction.

There is a buildup of negative charge on O₄ atom in each transition structure, consistent with C₅—O₄ (C_α—X) bond dissociation which increases on increasing the rate, according to the above observation that the C_α—X bond is dissociated to a larger degree in the faster reactions. The opposite trend is apparent in the buildup of positive charge on the transferred hydrogen, which decreases on increasing the rate, in agreement with the trend in C_β—H bond lengthening.^[36]

The average value, δB_{av}, is calculated as^[33]

$$\delta B_{av} = \frac{1}{n} \sum \delta B_i \quad (4)$$

with *n* being the number of bonds involved in the reaction, measures the degree of advancement of the transition state along the reaction path. Calculated δB_{av} values for the mechanism of the studied reaction are shown in Table 2. δB_{av} values are 0.47 and 0.46 for mechanisms (A) and (C), respectively, indicating that both transition states have an 'early' character, nearer to the reactants than to the products.

The synchronicity, S_y, of a chemical reaction can be calculated as

$$S_y = 1 - A \quad (5)$$

A being the asynchronicity, calculated using the expression proposed by Moyano *et al.*^[33]

$$A = \frac{1}{(2n - 2)} \sum \frac{|\delta B_i - \delta B_{av}|}{\delta B_{av}} \quad (6)$$

Synchronicities vary between 0 and 1, which is the case when all of the bonds implicated in the reaction center have broken or formed at exactly the same extent in the TS. The S_y values obtained in this way are, in principle, independent of the degree of advancement of the transition state. The S_y values calculated for the reactions studied are shown in Table 2. The synchronicities are 0.91 and 0.89, respectively for mechanism (A) and (C), indicating that the mechanisms correspond to highly asynchronous processes.

Asymmetrical charge distribution between C_α and C_β atoms in the transition structures (positively charged C_α and negatively charged C_β) also suggests asynchronous character in these reactions. The more polar the C_α—C_β bond, the faster is the reaction.

CONCLUSIONS

A theoretical study on the thermolysis of menthyl benzoate was carried out at the B3LYP/6-31 + G(d,p) and M05-2X/6-31 + G(d,p) level of theory. The results confirm that the mechanism is a *cis*-concerted elimination that occurs in one step, via a six-membered cyclic transition state. The transition state presents an 'early' character, nearer to the reactants than to the products. The breaking of the C_α—O bond is the more advanced process. The processes are highly asynchronous.

The M05-2X/6-31 + G(d,p)-calculated rate constants agree reasonably well with the available experimental values. The current study confirms the improved performance of the M05-2X functional as compared to B3LYP. Also, the theoretical results agree with the experimental fact that ratio of products **3ENE:2ENE** is approximately 2:1.

SUPPORTING INFORMATION

M05-2X/6-31G + (d,p) and B3LYP/6-31 + G(d,p)-calculated electronic energies, zero-point vibrational energies, thermal corrections to enthalpies, and entropies, for all the reactants, transition states, and products; Gibbs energy profile at 598.6 K, evaluated at the M05-2X/6-31 + G(d,p) level, for the thermal decomposition of menthyl benzoate; and M05-2X/6-31 + G(d,p)-optimized Cartesian coordinates for all the studied structures.

Acknowledgements

This work is supported by the research funds provided by Universidad Nacional de Colombia Sede Medellín. DIME Project: 20101006727 and the Spanish Ministerio de Ciencia e Innovación (Project CTQ2007-60895/BQU). E. Vélez is especially grateful to Dr Victor Polo for his valuable assistance in this work.

REFERENCES

- [1] F. Krafft, *Berichte Deutsch. Chem. Gesell.* **1883**, 16, 3018–3024.
- [2] R. T. Arnold, G. G. Smith, R. M. Dodson, *J. Org. Chem.* **1950**, 15, 1256–1260.
- [3] C. D. Hurd, F. H. Blunck, *J. Am. Chem. Soc.* **1938**, 60, 2419–2425.
- [4] H. R. Barton, *J. Chem. Soc.* **1949**, 2174–2178.
- [5] E. Vélez, J. Quijano, R. Notario, J. Murillo, J. F. Ramírez, *J. Phys. Org. Chem.* **2008**, 21, 797–807.
- [6] H. R. Barton, J. Head, R. J. Williams, *J. Chem. Soc.* **1953**, 1715–1719.
- [7] M. J. Frisch, G. W. Trucks, H. B. Schlegel, G. E. Scuseria, M. A. Robb, J. R. Cheeseman, J. A. Montgomery, Jr., T. Vreven, K. N. Kudin, J. C. Burant, J. M. Millam, S. S. Iyengar, J. Tomasi, V. Barone, B. Mennucci, M. Cossi, G. Scalmani, N. Rega, G. A. Petersson, H. Nakatsuji, M. Hada, M. Ehara, K. Toyota, R. Fukuda, J. Hasegawa, M. Ishida, T. Nakajima, Y. Honda, O. Kitao, H. Nakai, M. Klene, X. Li, J. E. Knox, H. P. Hratchian, J. B. Cross, V. Bakken, C. Adamo, J. Jaramillo, R. Gomperts, R. E. Stratmann, O. Yazyev, A. J. Austin, R. Cammi, C. Pomelli, J. W. Ochterski, P. Y. Ayala, K. Morokuma, G. A. Voth, P. Salvador, J. J. Dannenberg, V. G. Zakrzewski, S. Dapprich, A. D. Daniels, M. C. Strain, O. Farkas, D. K. Malick, A. D. Rabuck, K. Raghavachari, J. B. Foresman, J. V. Ortiz, Q. Cui, A. G. Baboul, S. Clifford, J. Cioslowski, B. B. Stefanov, G. Liu, A. Liashenko, P. Piskorz, I. Komaromi, R. L. Martin, D. J. Fox, T. Keith, M. A. Al-Laham, C. Y. Peng, A. Nanayakkara, M. Challacombe, P. M. W. Gill, B. Johnson, W. Chen, M. W. Wong, C. Gonzalez, J. A. Pople, *Gaussian 03, Revision E.01*, Gaussian, Inc., Wallingford, CT, **2004**.
- [8] W. Kohn, A. D. Becke, R. G. Parr, *J. Phys. Chem.* **1996**, 100, 12974–12980.

- [9] P. J. Stephens, F. J. Devlin, C. F. Chabalowski, M. J. Frisch, *J. Phys. Chem.* **1994**, *98*, 11623–11627.
- [10] Y. Zhao, N. E. Schultz, D. G. Truhlar, *J. Chem. Theory Comput.* **2006**, *2*, 364–382.
- [11] W. J. Hehre, L. Radom, P. V. R. Schleyer, J. A. Pople, *Ab Initio Molecular Orbital Theory*, Wiley, New York, **1986**.
- [12] A. D. Becke, *J. Chem. Phys.* **1993**, *98*, 5648–5652.
- [13] C. Lee, W. Yang, R. G. Parr, *Phys. Rev. B* **1988**, *37*, 785–789.
- [14] Y. Zhao, D. G. Truhlar, *Acc. Chem. Res.* **2008**, *41*, 157–167.
- [15] D. A. McQuarrie, J. D. Simon, *Molecular Thermodynamics*, University Science Books, Sausalito, CA, **1999**.
- [16] K. Fukui, *J. Phys. Chem.* **1970**, *74*, 4161–4163.
- [17] A. E. Reed, F. Weinhold, *J. Chem. Phys.* **1983**, *78*, 4066–4073.
- [18] A. E. Reed, L. A. Curtiss, F. Weinhold, *Chem. Rev.* **1988**, *88*, 899–926.
- [19] K. B. Wiberg, *Tetrahedron* **1968**, *24*, 1083–1096.
- [20] E. D. Glendening, A. E. Reed, J. E. Carpenter, F. Weinhold, *NBO, Version 3.1*, Madison, WI, (**1988**).
- [21] K. J. Glasstone, K. J. Laidler, H. Eyring, *The Theory of Rate Processes*, Chapter 4, McGraw-Hill, New York, **1941**.
- [22] S. W. Benson, *The Foundations of Chemical Kinetics*, McGraw-Hill, New York, **1969**.
- [23] C. Eckart, *Phys. Rev.* **1930**, *35*, 1303–1309.
- [24] C. J. Cramer, *Essentials of Computational Chemistry. Theories and Models*, John Wiley & Sons, Ltd., Chichester, **2002**.
- [25] S. Zhang, T. N. Truong, **2001**. *VKLab version 1.0*, University of Utah.
- [26] P. A. Scott, L. Radom, *J. Phys. Chem.* **1996**, *100*, 16502–16513.
- [27] W. P. Hu, D. G. Truhlar, *J. Am. Chem. Soc.* **1996**, *118*, 860–869.
- [28] Y. Zhao, N. González-García, D. G. Truhlar, *J. Phys. Chem. A* **2005**, *109*, 2012–2018.
- [29] J. Quijano, R. Notario, E. Chamorro, L. A. León, C. Sánchez, G. Alarcón, J. C. Quijano, G. Chuchani, *J. Phys. Org. Chem.* **2002**, *15*, 413–419.
- [30] E. Chamorro, J. Quijano, R. Notario, C. Sánchez, L. A. León, G. Chuchani, *Int. J. Quantum Chem.* **2003**, *91*, 618–625.
- [31] R. Notario, J. Quijano, L. A. León, C. Sánchez, J. C. Quijano, G. Alarcón, G. E. Chamorro, G. Chuchani, *J. Phys. Org. Chem.* **2003**, *16*, 166–174.
- [32] R. Notario, J. Quijano, C. Sánchez, E. Vélez, *J. Phys. Org. Chem.* **2005**, *18*, 134–141.
- [33] A. Moyano, M. A. Pericàs, E. Valentí, *J. Org. Chem.* **1989**, *54*, 573–582.
- [34] R. Taylor, G. G. Smith, W. H. Wetzel, *J. Am. Chem. Soc.* **1962**, *84*, 4817–4824.
- [35] R. Taylor, G. G. Smith, *Tetrahedron* **1963**, *19*, 937–947.
- [36] J. A. Erickson, S. D. Kahn, *J. Am. Chem. Soc.* **1994**, *116*, 6271–6276.